Thermal Ignition by Millimeter-Scale Surface Hot Spots

Donner T. Schoeffler and Joseph E. Shepherd
California Institute of Technology
Pasadena, CA, USA

1 Introduction

Predicting thermal ignition of flammable mixtures remains a challenge for hazard assessment in aviation. Lightning strike of an aircraft may result in intense localized heating and the formation of a hot spot on an internal surface [1]. Important to aviation safety is to assess the risk of thermal ignition if the hot spot forms in contact with a flammable mixture. Measurement of autoignition temperatures by the ASTM-E659 standardized test provides a deceptively low threshold temperature that can grossly underpredict temperatures for ignition by hot surfaces in external natural convective flows [2, 3]. Thermal ignition by heated surfaces has been studied by many researchers, however there is no universal theory or validated method of correlation such that ignition may be predicted for any given hot surface geometry and flammable mixture. Currently, individual hot surface and enclosure geometries must be investigated on a case-by-case basis. We are studying thermal ignition by millimeter-scale surface hot spots through laboratory experiments in order to make the essential measurements of thermal ignition temperature and its dependence on various parameters, such as hot spot size. In conjunction with experimental work, we have performed numerical simulations of a simplified model problem using one-step chemical kinetics in order to explore the basic dependence of thermal ignition temperature on the size and shape of a hot spot's temperature distribution. Numerical simulation methods and results are discussed here with experiments described in future work. Numerical simulations have previously been used to investigate thermal ignition in our labs, including a relevant study of thermal ignition by a glow plug using a similar, simplified model for analysis [4].

2 Simulation Methods

Numerical simulations were performed using the open-source CFD toolbox OpenFOAM-9. A solver native to the toolbox, `buoyantReactingFoam`, was used for this study. The relevant equation set is

$$\frac{\partial \rho}{\partial t} + \nabla \cdot (\rho \mathbf{u}) = 0 \tag{1}$$

$$\frac{\partial \rho \mathbf{u}}{\partial t} + \nabla \cdot (\rho \mathbf{u}\mathbf{u}) = -\nabla P + \rho \mathbf{g} + \nabla \cdot \tau \tag{2}$$

$$\frac{\partial \rho (h_s + |\mathbf{u}|^2/2)}{\partial t} + \nabla \cdot (\rho \mathbf{u}(h_s + |\mathbf{u}|^2/2)) = \nabla \cdot (\lambda / c_P \nabla h_s) + \frac{\partial P}{\partial t} + \dot{q}_c \tag{3}$$

$$\frac{\partial \rho Y_i}{\partial t} + \nabla \cdot (\rho \mathbf{u} Y_i) = -\nabla \cdot \mathbf{j_i} + \dot{\Omega}_i \, . \tag{4}$$

Correspondence to: dschoeff@caltech.edu

In Equations (1)-(4), h_s is the sensible enthalpy, λ is the thermal conductivity, c_P is the specific heat capacity at constant pressure, $\mathbf{j}_i$ is the diffusive mass flux of species i, $\dot{q}_c$ is the rate of heat addition by chemical reaction, $\dot{\Omega}_i$ is the production rate for species i, and τ is the viscous stress tensor,

$$\tau = \mu(\nabla\mathbf{u} + (\nabla\mathbf{u})^T) - \frac{2}{3}\mu(\nabla\cdot\mathbf{u})\mathbf{I} \,. \tag{5}$$

The fluid was modeled as a mixture of two perfect gases, describing a reactant and product species with a single irreversible reaction, $\mathcal{R} \rightarrow \mathcal{P}$. The gas thermodynamic and transport properties were chosen to model a stoichiometric hexane-air mixture at 1 bar and 300 K. The resulting specific heat ratios were $\gamma_\mathcal{R} = 1.262$ and $\gamma_\mathcal{P} = 1.266$ for the reactant and product species, respectively. The heat release was $q_c = 2.791$ MJ/kg, and a molecular weight of 30.09 kg/kmol was used for both species. Thermodynamic calculations were implemented in OpenFOAM using NASA7 polynomials [5, 6]. Fick's law with unity Lewis number was used for species diffusion, such that $\mathbf{j}_\mathcal{R} = -\lambda/c_P\nabla Y_\mathcal{R}$. Sutherland's law, $\mu = A_s\sqrt{T}/(1+T_s/T)$, and a modified Eucken relation, $\lambda = \mu c_v(1.32+1.77R/c_v)$, were used to compute temperature-dependent viscosity and thermal conductivity, respectively, and the relevant constants were $A_s = 1.52\cdot10^{-6}$ [kg m^{-1}s^{-1}K$^{-1/2}$] and $T_s = 148$ [K].

The one-step reaction mechanism was specified using a modified-Arrhenius rate law,

$$k(T) = AT^\alpha \exp\left(-E_a/\tilde{R}T\right) \,. \tag{6}$$

The constants were determined using a method described by Melguizo-Gavilanes [4], where they were used to fit ignition delay times from constant-pressure adiabatic explosion calculations using the detailed mechanism JetSurF 2.0 [7]. The resulting constants are $A = 0.3$ K$^{-\alpha}$s^{-1}, $\alpha = 2.7$, and $T_a = 17986.576$ K, where T_a is the activation temperature, $T_a = E_a/\tilde{R}$.

An axisymmetric simulation domain was used for all calculations with domain radius and height equal to ten times the relevant hot spot radius. Adequate grid resolution was obtained with a minimum cell size of 25 μm at the hot spot center. A geometric progression both radially and axially with rate of 1.006 was used to expand cells away from the hot spot and reduce grid density far from the hot spot. Boundary conditions were chosen to model a closed domain with the no-slip condition at all walls. The side and top walls had isothermal 300 K boundary conditions. The hot spot was modeled as a time-varying boundary condition on the bottom wall of the domain. Two hot spot temperature distributions were studied: a top-hat and Gaussian shapes. The simulated hot spot sizes were 3, 4, 5, 7, and 10 mm, where the size refers to the full width at half maximum (FWHM) for the Gaussian hot spots. The hot spot temperature, T_{HS}, is the peak temperature of the distribution. The amplitude of both distributions was ramped linearly with time initially from the ambient temperature of 300 K at a rate of 200 K/s until after ignition occurred for all simulated cases.

3 Results and Discussion

The natural convective flow field that forms above the hot spot when chemical reaction remains negligible is illustrated in Figure 1 for a 5 mm top-hat hot spot. Gas in contact with the hot spot is heated to high temperature, which expands and drives a buoyant plume upward. The plume entrains surrounding cold gas and substantially cools down. Consequently, the region of highest temperature in the domain occurs directly adjacent to the hot spot in a nearly stagnant layer. Ignition occurs in a region of this layer on the domain centerline for all simulations.

Figure 2 plots the evolution of temperature and reaction progress along the domain centerline for the 5 mm top-hat hot spot as its temperature increases. For early time, hot spot temperatures are low and

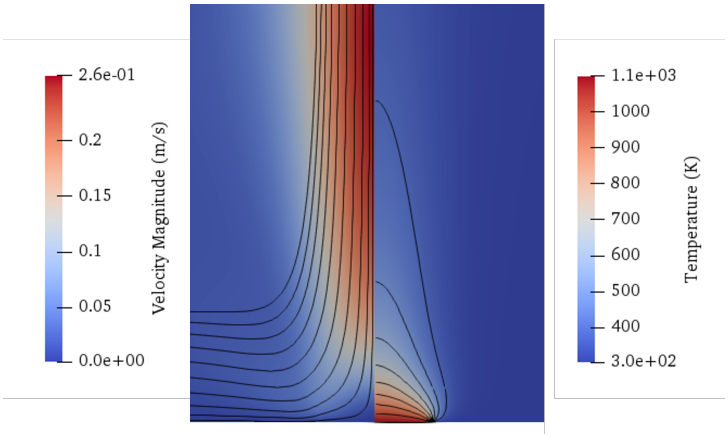

Figure 1: Contours of velocity and temperature fields on left and right halves, respectively, for 5 mm top-hat hot spot at time $t = 4.0$ s and temperature $T = 1100$ K. Image shows cropped view of entire simulation domain

heat addition from chemical reaction is negligible, and so heat only diffuses from the hot spot. At larger temperatures, the rate of chemical reaction is sufficient for heat addition to begin competing with heat loss, and the near wall temperature gradient decreases. As the reaction rate increases, diffusion cannot completely replace burned reactants, and there is a local net reactant depletion. At sufficiently high temperatures, the rate of heat addition balances heat loss to the colder surrounding gas, and the temperature gradient goes to zero at the wall. This point of adiabaticity is often referred to as the van't Hoff ignition criterion, however, ignition occurs in all cases only after additional increase in temperature. At the point of adiabaticity, flame temperatures remain much greater than wall temperatures, such that when a flame forms there is necessarily large heat loss back to the wall. Proximity with the wall therefore quenches flame formation until the point of maximum temperature is displaced sufficiently far from the wall such that the rate of heat addition exceeds both losses to the cool ambient gas and to the wall. This description of the hot surface ignition phenomenon has been observed numerous times by previous studies using numerical simulations [4, 8–10].

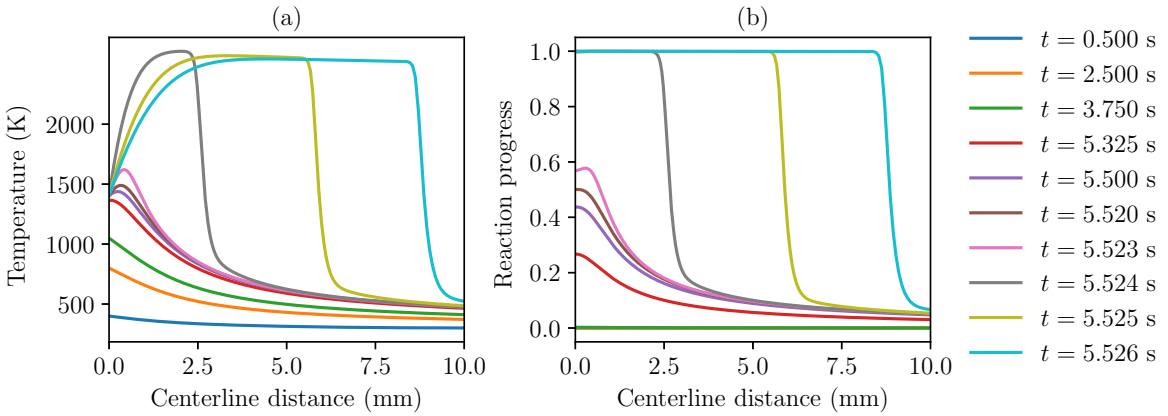

Figure 2: (a) temperature and (b) reaction progress plotted along the domain centerline for the 5 mm top-hat hot spot at various time steps before and after ignition

When ignition occurs, the maximum temperature in the domain rapidly increases at a rate much greater than the heating rate of the wall. This does not occur until after the wall temperature has increased some

amount past the van't Hoff condition. The criterion chosen to identify ignition is the time when the maximum temperature in the domain exceeds the peak wall temperature by 150 K, a criterion successfully used in previous numerical simulations [4, 9]. The ignition temperature is then identified as the wall temperature when ignition occurs. Figure 3(a) plots the resulting ignition temperatures for all simulated hot spot sizes. The strong inverse trend is consistent with previous studies of surface hot spots [11] and stationary heated particles [12]. Figure 3(b) shows the difference between ignition temperatures and the wall temperature at the van't Hoff criterion, illustrating that the difference between criteria increases as the hot spot size decreases. However, the difference is small relative to the ignition temperature, and the van't Hoff criterion underpredicts the ignition temperature by less than 6% for all of the simulated cases.

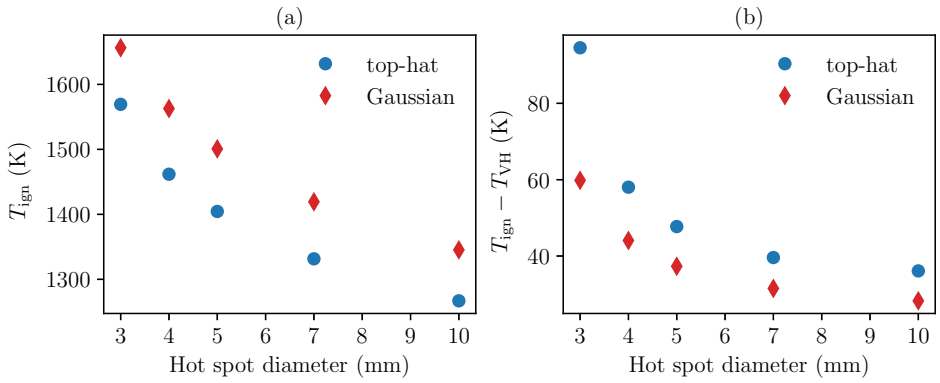

Figure 3: (a) hot spot temperature at ignition, T_{ign}, for simulated hot spot diameters, where diameter for Gaussian refers to FWHM. (b) difference between wall temperature at ignition and when van't Hoff criterion is reached, T_{VH}

Generally, thermal ignition occurs when a balance between modes of heat addition and heat loss allows further self heating to cause thermal runaway. Ignition by surface hot spot occurs in the hot gas layer confined directly adjacent to the surface. Buoyant convection is important for establishing the temperature field in which ignition occurs, however the heated gas layer is nearly stagnant and dominated by diffusive processes. Adler [13] performed a Frank-Kamenetskii-type stability analysis [14] of a stagnant combustible layer heated by a surface hot spot, deriving a critical Frank-Kamenetskii parameter. However, further work is required to relate his assumed temperature profile and slab scaling with the temperature fields produced by various surface hot spots.

Correlations for hot surface ignition have been derived by several authors, including Khitrin and Goldenberg [15], Ono et al. [16], and Laurendeau [17], where all authors typically model a system in which diffusive heat loss is balanced by chemical heat addition, and hence derive similar results. The resulting correlations typically give an inverse-log relation between a characteristic length scale and an ignition temperature, i.e., $\log(L) \propto T_{\mathrm{ign}}^{-1}$. The heated surface size provides the characteristic length to describe heat transfer to the gas, however the length scale is particular to the surface geometry, and so it is not translatable between different geometries or heated surface temperature distributions. Instead, a more general length scale can be derived from a characteristic thickness of the thermal layer itself, which forms adjacent to the heated surface. A characteristic thermal layer thickness, Λ, is given by the inverse of a normalized temperature gradient at the wall, i.e.,

$$\Lambda = \left(\frac{c_P}{q_c} \left| \frac{\partial T}{\partial z} \right|_{z=0} \right)^{-1}, \tag{7}$$

where the ratio of heat release and specific heat capacity, q_c/c_P, normalize the temperature. The ap-

propriate thermal layer thickness to describe the hot surface ignition problem is Λ, evaluated for a *chemically-frozen* flow at the time and position of ignition.

The justification for modeling hot surface ignition with a frozen natural convective flow is in formulating it as a boundary layer problem, solved using methods of matched-asymptotic expansions as developed by many authors [18–24]. With large activation energy asymptotics, the outer flow is well approximated as chemically frozen, and reaction only occurs in a near-wall reactive-diffusive inner problem. The relevant heat transfer parameter is the wall temperature gradient given by the frozen outer flow [20]. First-order matched-asymptotic analysis derives an ignition criterion in the form of a critical Dahmköhler number, which is reached when adiabaticity occurs at the wall, i.e., the van't Hoff condition. Law [19] asserted that the observation that ignition occurs in numerical simulations only when a temperature maximum forms displaced from the wall is purely a second order phenomenon, although this remains to be validated. The critical Dahmköhler number derived by Law [20], assuming zero reactant depletion, can be reformulated in terms of a critical thermal layer thickness to give

$$\begin{aligned}\Lambda_{\text{crit}} &= \left[2\frac{c_P}{q_c}\frac{\rho_w}{\lambda/c_P}\frac{T_w^2}{T_a}AT_w^{\alpha}e^{-T_a/T_w}\right]^{-1/2} \\ &= l_K/\sqrt{2}\,,\end{aligned} \tag{8}$$

where l_K is a characteristic thickness of the ignition kernel, a length scale equivalent to a flame thickness evaluated at the wall temperature instead of the flame temperature.

The result (8) motivates a method for correlating the present simulation data. Figure 4(a) shows l_K plotted against the thermal layer thickness Λ, where both are evaluated at the van't Hoff condition. The frozen thermal layer thickness was computed on the domain centerline at the van't Hoff condition by interpolating forward from early simulation time when chemical reactions were negligible at the wall. Figure 4(a) shows that data for both top-hat and Gaussian hot spots collapse to a single line. The linear fit is constrained to a zero intercept, giving $l_K = 0.885\Lambda_{\text{VH}}$. Residuals are plotted in Figure 4(b) illustrating that there remains some small, yet systematic error, which suggests that there is additional relevant scaling not captured by the model. An essential factor that has not been incorporated in this correlation is the significant reactant depletion that occurs at the hot spot prior to ignition as illustrated in Figure 2(b).

The thermal layer thickness provides a natural method for describing an equivalent hot spot size for varying temperature profiles. Figure 5 illustrates how Λ_{VH} scales with nominal hot spot diameters. From the two linear fits, a conversion relation between the top-hat and Gaussian hot spots follows directly,

$$D_{\text{G}} = 1.859D_{\text{TH}} - 0.700\ [\text{mm}]\,, \tag{9}$$

where D_{TH} is the top-hat diameter and D_{G} is the Gaussian FWHM. The equivalent hot-spot temperature profiles are plotted in Figure 6, illustrating that the rapid radial drop off in temperature of the Gaussian profile requires a correspondingly much broader hot spot to achieve ignition at similar temperatures to a top-hat hot spot.

Future work will extend the range of hot spot geometries to further evaluate the quality of the correlations and their domain of applicability. Only correlations with the van't Hoff criterion were discussed, and it remains to extend the above methods to model the true wall temperature at which ignition occurs.

Acknowledgements This work was supported by The Boeing Company through a Strategic Research and Development Relationship Agreement CT-BA-GTA-1.

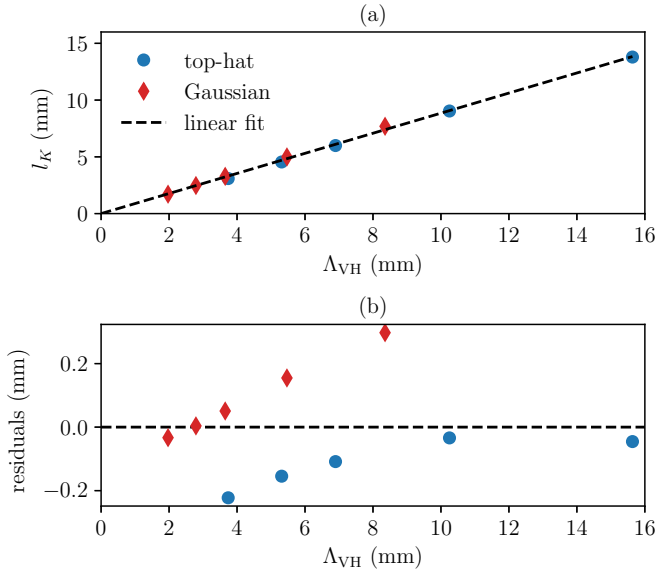

Figure 4: In (a), the ignition kernel thickness, l_K, is plotted against thermal layer thickness, Λ_{VH}, where both are evaluated at the van't Hoff condition. Residuals between simulation data and constrained zero-intercept linear fit are shown in (b)

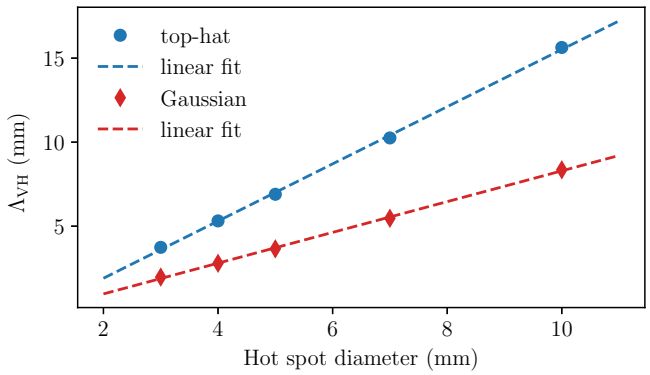

Figure 5: Correlation between Λ_{VH} and hot spot diameters. Linear fits for top-hat and Guassian data are, respectively, $y = 1.702x - 1.503$ and $y = 0.915x - 0.863$

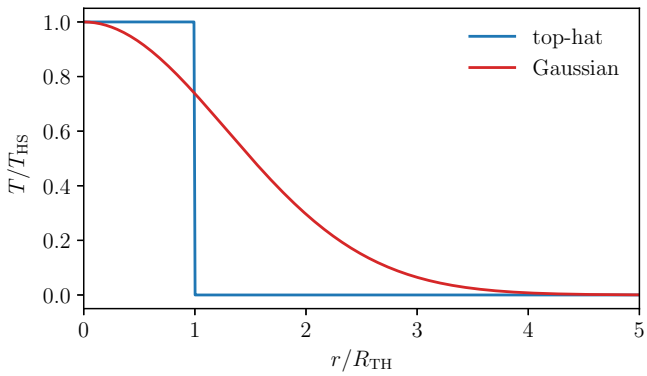

Figure 6: Equivalent top-hat and Gaussian hot spots, where radial coordinate is normalized by the top-hat radius, R_{TH}, and temperature is normalized by the hot spot temperature, T_{HS}

References

[1] L. Chemartin, P. Lalande, B. Peyrou, A. Chazottes, P. Elias, C. Delalondre, B. Cheron, and F. Lago, "Direct Effects of Lightning on Aircraft Structure: Analysis of the Thermal, Electrical and Mechanical Constraints," *Aerospace Lab*, no. 5, pp. p. 1–15, Dec. 2012. [Online]. Available: https://hal.science/hal-01184416

[2] C. D. Martin and J. E. Shepherd, "Low temperature autoignition of Jet A and surrogate jet fuel," *Journal of Loss Prevention in the Process Industries*, vol. 71, p. 104454, Jul. 2021. [Online]. Available: https://www.sciencedirect.com/science/article/pii/S0950423021000656

[3] S. Jones and J. Shepherd, "Thermal ignition by vertical cylinders," *Combustion and Flame*, vol. 232, p. 111499, Oct. 2021. [Online]. Available: https://www.sciencedirect.com/science/article/pii/S001021802100242X

[4] J. Melguizo-Gavilanes, A. Nové-Josserand, S. Coronel, R. Mével, and J. E. Shepherd, "Hot Surface Ignition of *n* -Hexane Mixtures Using Simplified Kinetics," *Combustion Science and Technology*, vol. 188, no. 11-12, pp. 2060–2076, Dec. 2016. [Online]. Available: https://www.tandfonline.com/doi/full/10.1080/00102202.2016.1212577

[5] B. J. McBride, S. Gordon, and M. A. Reno, "Coefficients for Calculating Thermodynamic and Transport Properties of Individual Species," NASA, Technical Memorandum TM-4513, 1993.

[6] S. T. Kao, "Detonation Stability with Reversible Kinetics," Ph.D. dissertation, California Institute of Technology, Pasadena, California, 2008.

[7] H. Wang, E. Dames, B. Sirjean, D. A. Sheen, R. Tango, A. Violi, J. Y. W. Lai, F. N. Egolfopoulos, D. F. Davidson, R. K. Hanson, C. T. Bowman, C. K. Law, W. Tsang, N. P. Cernansky, D. L. Miller, R. P. Lindstedt, "A high-temperature chemical kinetic model of n-alkane (up to n-dodecane), cyclohexane, and methyl-, ethyl-, n-propyl and n-butyl-cyclohexane oxidation at high temperatures, JetSurF version 2.0," Sep. 2010. [Online]. Available: http://web.stanford.edu/group/haiwanglab/JetSurF/JetSurF2.0/index.html

[8] L.-D. Chen and G. M. Faeth, "Ignition of a combustible gas near heated vertical surfaces," *Combustion and Flame*, vol. 42, pp. 77–92, Jan. 1981. [Online]. Available: https://www.sciencedirect.com/science/article/pii/0010218081901437

[9] S. A. Coronel, S. Lapointe, and J. E. Shepherd, in *Proceedings of the 11th U.S. National Combustion Meeting*, 2019.

[10] S. M. Jones, "Thermal Ignition by Vertical Cylinders," Ph.D. dissertation, California Institute of Technology, 2021.

[11] D. Rae, B. Singh, and R. Danson, "The Size and Temperature of a Hot Square in a Cold Plane Surface Necessary for the Ignition of Methane," Ministry of Power, Safety in Mines Research, Research Report 224, 1964.

[12] D. Roth, P. Sharma, T. Haeber, R. Schiessl, H. Bockhorn, and U. Maas, "Ignition by Mechanical Sparks: Ignition of Hydrogen/Air Mixtures by Submillimeter-Sized Hot Particles," *Combustion Science and Technology*, vol. 186, no. 10-11, pp. 1606–1617, Nov. 2014. [Online]. Available: http://www.tandfonline.com/doi/abs/10.1080/00102202.2014.935606

[13] J. Adler, "Ignition of a combustible stagnant gas layer by a circular hot-spot," *Combustion Theory and Modelling*, vol. 3, no. 2, pp. 359–369, Jun. 1999. [Online]. Available: http://www.tandfonline.com/doi/abs/10.1088/1364-7830/3/2/309

[14] D. Frank-Kamenetskii, *Diffusion and Heat Exchange in Chemical Kinetics*. Princeton University Press, 1955.

[15] L. Khitrin and S. Goldenberg, "Thermal theory of ignition of gas mixtures: Limiting conditions," *Symposium (International) on Combustion*, vol. 6, no. 1, pp. 545–554, Jan. 1957. [Online]. Available: https://linkinghub.elsevier.com/retrieve/pii/S0082078457800721

[16] S. Ono, H. Kawano, H. Niho, and G. Fukuyama, "Ignition in a Free Convection from Vertical Hot Plate," *Bulletin of JSME*, vol. 19, no. 132, pp. 676–683, 1976.

[17] N. M. Laurendeau, "Thermal ignition of methane-air mixtures by hot surfaces: A critical examination," *Combustion and Flame*, vol. 46, pp. 29–49, Jan. 1982. [Online]. Available: https://linkinghub.elsevier.com/retrieve/pii/0010218082900050

[18] C. K. Law, "Ignition of a Combustible Mixture by a Hot Particle," *AIAA Journal*, vol. 16, no. 6, pp. 628–630, Jun. 1978. [Online]. Available: https://arc.aiaa.org/doi/10.2514/3.7561

[19] ——, "On the stagnation-point ignition of a premixed combustible," *International Journal of Heat and Mass Transfer*, vol. 21, no. 11, pp. 1363–1368, Nov. 1978. [Online]. Available:

https://www.sciencedirect.com/science/article/pii/0017931078901990

[20] ——, *Combustion Physics*. Cambridge: Cambridge University Press, 2006. [Online]. Available: https://www.cambridge.org/core/books/combustion-physics/8259DA7A712262E03DD72C365F89F32E

[21] A. Liñán and F. A. Williams, "Ignition of a Reactive Solid Exposed to a Step in Surface Temperature," *SIAM Journal on Applied Mathematics*, vol. 36, no. 3, pp. 587–603, Jun. 1979. [Online]. Available: http://epubs.siam.org/doi/10.1137/0136042

[22] F. Mendez, C. Treviño, and A. LiÑÁNE, "Premixed Combustion in Boundary Layers for Moderate Values of the Zeldovich Numbers," *Combustion Science and Technology*, vol. 48, no. 3-4, pp. 129–149, Jul. 1986. [Online]. Available: http://www.tandfonline.com/doi/abs/10.1080/00102208608923889

[23] C. Treviño and F. Méndez, "Asymptotic Analysis of the Ignition of Hydrogen by a Hot Plate in a Boundary Layer Flow," *Combustion Science and Technology*, vol. 78, no. 4-6, pp. 197–216, Aug. 1991. [Online]. Available: http://www.tandfonline.com/doi/abs/10.1080/00102209108951749

[24] A. K. Kapila, *Asymptotic Treatment of Chemically Reacting Systems*. Pitman Publishing Inc, 1983.